

Conformational Ensemble View of G Protein-Coupled Receptors and the Effect of Mutations and Ligand Binding

Ravinder Abrol^{*,1}, Soo-Kyung Kim^{*}, Jenelle K. Bray[†],
Bartosz Trzaskowski[‡], William A. Goddard III^{*,1}

^{*}Materials and Process Simulation Center, California Institute of Technology, Pasadena, California, USA

[†]Department of Structural Biology, Stanford Medical School, Stanford, California, USA

[‡]Faculty of Chemistry, University of Warsaw, Warsaw, Poland

¹Corresponding authors: e-mail address: abrol@wag.caltech.edu; wag@wag.caltech.edu

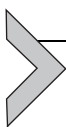
Contents

1. Introduction	32
2. Overview of the Conformational Ensemble Prediction	35
3. Generating Starting Structures Based on Templates	36
4. BiHelix: TM Bundle Conformational Sampling of Helix Rotation Angles	38
5. SuperBiHelix TM Bundle Sampling of All Helix Orientation Angles	40
6. Effect of Mutations on the WT Conformational Ensemble	41
7. Ensemble Docking of Ligands to WT or Mutant Receptors	42
7.1 Ensemble docking of agonists and antagonists to human A ₃ adenosine receptor	42
7.2 Ensemble ligand docking to human CCR5 chemokine receptor mutants	45
8. Summary	46
Acknowledgments	46
References	46

Abstract

G protein-coupled receptors (GPCRs) are integral membrane proteins that can convert an extracellular signal into multiple intracellular signaling processes. This pleiotropy of GPCRs is enabled by their structural flexibility manifested in thermally accessible multiple conformations, each of which may be capable of activating a different signaling cascade inside the cell (Kenakin & Miller, 2010). Different subsets of conformations can be potentially stabilized through mutations, or binding to various ligands (inverse agonists, antagonists, and agonists), or binding to G proteins, etc. Structure determination efforts have led to a small subset of these receptors being crystallized in one or two distinct conformations, but computational methods can predict an ensemble of conformations that characterize the full thermodynamic landscape of the receptor.

Mutations in the receptor or binding of ligands can modulate this energy landscape, by stabilizing a unique set of conformations under different conditions, which may correspond to a specific downstream physiological function. These studies can provide testable hypotheses on the structural basis of GPCR activation and functional selectivity.



1. INTRODUCTION

G protein-coupled receptors (GPCRs) are integral membrane proteins that are used by cells to convert extracellular signals (e.g., ligand binding) into intracellular responses (Abrol & Goddard, 2011; Rosenbaum, Rasmussen, & Kobilka, 2009). These receptors form a superfamily of membrane proteins comprising of structurally diverse five distinct families (Lagerstrom & Schioth, 2008) that are capable of sensing an extremely diverse set of signals (from photons to small molecules to large proteins). However, they all share the common structural motif of seven-transmembrane helices (TMHs) connected by three extracellular loops and three intracellular loops. Due to the critical role played by these receptors in cellular signaling, they are the target of more than half of the drugs in the market or under development (Lagerstrom & Schioth, 2008).

GPCRs have evolved into pleiotropic machines, wherein each receptor can potentially control multiple intracellular signaling pathways. They were originally discovered to control G protein-mediated pathways, which gave them their original name. Overwhelming evidence has shown that they can also trigger G protein independent pathways, for example, via β arrestins (Rajagopal, Lefkowitz, & Rockman, 2005; Shukla, Xiao, & Lefkowitz, 2011), suggesting that they should be referred to as 7TM receptors. Their pleiotropic nature is caused by a remarkable level of conformational flexibility. This enables these receptors to be stabilized into a specific conformation or a subset of conformations depending on the physiological conditions (e.g., agonist ligand binding, G protein binding, etc.) which can then trigger a very specific intracellular response or a set of responses (Kenakin & Miller, 2010). This, in turn, makes these receptors capable of biased signaling, where a specific ligand may be designed to activate only one intracellular pathway (Kenakin, 2012). This has critical implications for drug discovery where a known drug candidate for a GPCR target may activate two intracellular pathways: one therapeutically beneficial and another undesirable that can cause side effects. A well-known example of this is the GPR109A receptor, whose agonist ligand niacin acts therapeutically as an antilypolytic agent via

G protein-mediated pathways, but causes cutaneous flushing as a major side effect which has been directly linked to the activation of the β arrestin 1 pathways (Walters et al., 2009). A structural analog of this molecule that selectively blocks the coupling to β arrestin 1 pathway would be highly desirable.

The structural biology of these receptors has seen an exciting exponential progress in the past several years (Tate & Stevens, 2010) due to a major revolution in membrane protein structure determination methods (Blois & Bowie, 2009). Several receptors have now been crystallized in two major structurally different conformations putatively associated with the inactive state and the G protein-coupled active state, highlighting the large conformational changes that these receptors are capable of (Abrol, Kim, Bray, Griffith, & Goddard, 2011). Combining these structural insights with functional studies and a thermodynamic view of protein conformations, an energy landscape picture is emerging for these receptors (Deupi & Kobilka, 2010), that aims to provide a dynamic view of these receptors when confronted with different physiological conditions.

Figure 2.1 captures this emerging dynamic energy landscape of these receptors (Abrol et al., 2011), where I refers to the inactive conformation for a receptor, putatively most stable in the wild-type (WT) receptors; C

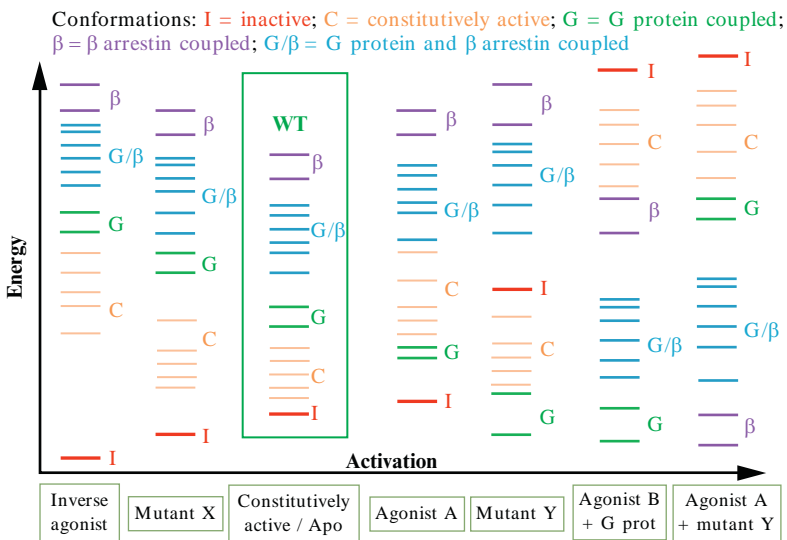


Figure 2.1 Functional and thermodynamic view of GPCR conformational ensembles (Abrol et al., 2011).

refers to the conformations that are thermally accessible for basally active receptors; G refers to conformations that can exclusively couple to G proteins; β refers to conformations that can exclusively couple to β arrestins; and “G/ β ” refers to conformations that can couple to both G proteins and β arrestins. This figure depicts the conformations of a single GPCR in the increasing order of energy along the y -axis. The x -axis loosely resembles a mean or collective activation pathway for the receptor under different conditions from left to right, where the leftmost form of the receptor is fully inactive and the rightmost form can couple to β arrestins. For a given form of the receptor, only the conformations close to the lowest energy conformation will be thermally accessible, and their relative population will be determined by the Boltzmann factor. The receptor ensembles depicted in Fig. 2.1 provide a conformational ensemble framework to conceptualize the dynamical nature of GPCRs in the cell membrane when faced with different physiological conditions. All GPCRs (including mutants and different subtypes) are expected to have a unique ensemble of conformations. Figure 2.1 also depicts how potential changes in a conformational ensemble might compare for a WT and mutant receptor, in the event that the mutation(s) lead to inactivation or a constitutively active receptor protein. Additionally, it depicts how functionally distinct receptor conformations might be stabilized under different conditions (e.g., agonist binding, inverse agonist binding, G protein binding, etc.).

Structure determination efforts are providing discrete information on these functionally distinct conformations and computational methods have a vital role to play in complementing these efforts by providing a dynamic and energetic framework to characterize the functionally distinct conformations. Molecular dynamics (MD) simulations are unable to bridge the transition between inactive and multiple active conformations for two reasons: first, the time scales involved are in the range of milliseconds to seconds and second, besides the active conformations being energetically uphill, there will be significant barriers that can only be overcome through rare events in the simulations. Monte Carlo (MC)-based methods can overcome these issues by being able to predict potentially all thermally accessible conformations for a receptor as long as the conformational space is exhaustively sampled. This work describes the use of one such method GEnSeMBLE (GPCR Ensemble of Structures in Membrane BiLayer Environment) developed to predict the conformational ensembles of GPCRs under specific conditions of receptor mutants and/or ligand binding. The GEnSeMBLE procedure brings together methods for TM helix region prediction, helix

shape optimization, and exhaustive but efficient TM helix bundle conformational sampling (Abrol, Griffith, Bray, & Goddard, 2012). This exhaustive sampling predicts an ensemble of low-energy GPCR conformations expected to play different functional roles in GPCR-mediated signaling pathways. The next section provides an overview and the implementation sequence of the key parts of this method. It is followed by sections detailing the steps involved in each of those parts along with typical results to show how the predicted conformations are interpreted.



2. OVERVIEW OF THE CONFORMATIONAL ENSEMBLE PREDICTION

For a target GPCR, whose conformations need to be determined in the apo form [for both WT and mutants] and/or the holo form [in the presence of different ligands, say, agonists, neutral antagonists, inverse agonists, and allosteric modulators], the following sequence of different methods is implemented:

- 2.1. A starting structure is obtained for the WT receptor using multiple templates (both experimental and previously predicted ones) as described in [Section 3](#). That section also provides a definition of the TM bundle orientation parameters in terms of TM helix positions and angles (tilt, sweep, and rotation angles) used to characterize a given template, or any conformation (experimental or predicted).
- 2.2. These different starting structures are taken through a complete sampling of all combinations of helix rotation angles (~ 35 million TM bundle conformations sampled) as described in [Section 4](#). The top structure (s) from templates resulting in lowest energy conformations are selected.
- 2.3. The selected conformations are then used as starting structures for an exhaustive sampling of all combinations of helix tilt and sweep angles in addition to helix rotation angles (~ 10 trillion TM bundle conformations sampled) as described in [Section 5](#). The ensemble of top 100 most stable receptor conformations are selected for studying the effect of various mutations and binding of different ligands.
- 2.4. To predict an ensemble of conformations for a given mutant, the top 100 WT conformations are mutated, optimized, and reordered by energy to obtain a new ordering of receptor conformations corresponding to a specific mutant as described in [Section 6](#).
- 2.5. To obtain WT or mutant receptor conformations preferred by a ligand, the top 20 receptor conformations from the WT conformational

ordering or the mutant conformational ordering are docked to multiple torsional conformers of the ligand as described in [Section 7](#).



3. GENERATING STARTING STRUCTURES BASED ON TEMPLATES

GPCRs are characterized by seven roughly parallel TM helices oriented perpendicular to the membrane plane. To characterize this 7TM bundle topology uniquely requires the specification of six orientation parameters for each of the seven TM helices ([Abrol et al., 2011](#)). These orientation parameters also require a unique definition of the helical axis, which is defined as the least moment of inertia axis vector obtained by the eigensolution of the moment of inertia matrix for the helix in question using only its heavy backbone atoms. The TM helices can be kinked due to proline residues, but this definition provides a unique helical axis for such helices as well. The six helix orientation parameters are shown in [Fig. 2.2](#) and defined as follows: “ h ” refers to the hydrophobic center residue that would correspond to the helix residue residing exactly at the membrane middle (also referred to as the membrane hydrophobic plane); “ x ” and “ y ” refer to the position of this hydrophobic center residue on the membrane hydrophobic plane; “ θ ” corresponds to the tilt angle of the helical axis (defined above) relative to the membrane normal, which is assumed to be the z -axis; “ ϕ ” refers to the helix sweep angle that specifies the direction of the helical axis tilt; and “ η ” refers to the helix rotation angle about its own axis. This rotation angle is defined by the position of the $C\alpha$ atom of the most conserved residue in each TM helix [residue $j.50$ for the TM helix j using the Ballesteros convention ([Ballesteros & Weinstein, 1995](#)), except for TM3 for which residue 3.32 is used].

As mentioned in [Section 1](#), there has been an exponential increase in GPCR crystal structures, which is also slowly expanding in sequence space. These structures are viable templates for homology models, which serve as

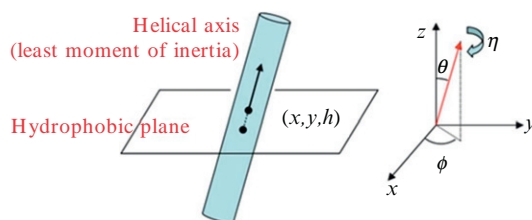


Figure 2.2 Definition of helix orientation parameters ([Abrol, Bray, & Goddard, 2012](#)).

starting structures for the subsequent conformational sampling procedures. In addition to these experimental structures, we have some predicted GPCR structures which have been relaxed in their physiological membrane environment by MD simulations. The following structures are currently available as templates to predict inactive conformations:

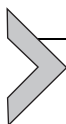
1. Bovine rhodopsin (Palczewski et al., 2000).
2. Human $\beta 2$ adrenergic receptor (Cherezov et al., 2007).
3. Turkey $\beta 1$ adrenergic receptor (Warne et al., 2008).
4. Human A_{2A} adenosine receptor (Jaakola et al., 2008).
5. Human D_3 dopamine receptor (Chien et al., 2010).
6. Human $CXCR_4$ chemokine receptor (Wu et al., 2010).
7. Human H_1 histamine receptor (Stevens et al., 2011).
8. Human M_2 muscarinic acetylcholine receptor (Haga et al., 2012).
9. Human M_3 muscarinic acetylcholine receptor (Kruse et al., 2012).
10. Human $S1P_1$ sphingosine-1-phosphate receptor (Hanson et al., 2012).
11. The predicted structure for the human $CCR1$ receptor with an antagonist BX 471 bound that was subjected to 10 ns of MD using an infinite membrane and full solvent (Vaidehi et al., 2006).
12. The predicted structure for the DP receptor with the CDP_2 agonist bound that was subjected to 2 ns of MD using an infinite membrane and full solvent (Li et al., 2007).
13. The predicted structure for the $MrgC11$ receptor with an agonist FdMRFa bound that was subjected to 7 ns of MD using an infinite membrane and full solvent (Heo et al., 2007).

The following structures are currently available as templates to predict the active GPCR conformations:

1. Bovine meta rhodopsin II (Choe et al., 2011).
2. Human $\beta 2$ adrenergic receptor bound to an agonist and Gs protein (Rasmussen et al., 2011).
3. Human A_{2A} adenosine receptor bound to an agonist (Xu et al., 2011).

The six orientation parameters for the TM helices in the templates are obtained by first rotating the membrane-aligned receptors [obtained from the OPM database (Lomize, Lomize, Pogozheva, & Mosberg, 2006) for the experimental templates and from the MD simulations in the membrane for the predicted templates] in the x - y plane such that the helical axis of TM helix 3 goes through the origin, and that of TM helix 2 intersects the x -axis. When this transformation is coupled to the convention that the extracellular face of the receptor points in the $+z$ direction, a unique set of orientation parameters are obtained. All of the above-mentioned templates can be used

to generate starting structures for the GEnSeMBLE conformational sampling protocol. This starting structure is essentially a homology model of the target GPCR based on mutating a specific template. If a target GPCR structure has a sequence similarity higher than $\sim 60\%$ in the TM regions to one of these templates, that template will typically result in the lowest energy conformations after conformational sampling using GEnSeMBLE.



4. BIHELIX: TM BUNDLE CONFORMATIONAL SAMPLING OF HELIX ROTATION ANGLES

Using the starting structure from the previous step, a full conformational space sampling is performed in the helix rotation angle η space using the BiHelix procedure (Abrol, Bray, et al., 2012). For each of the seven TM helices, if one samples the full rotation angle space on a 30° grid, it will result in $12^7 \sim 35$ million TM bundle conformations, for each of which the residue side chains need to be optimized to obtain the most favorable interactions across the TM bundle being sampled. This becomes computationally very prohibitive quickly, especially when one needs to sample other degrees of freedom like helix tilt and sweep angles as well. The following BiHelix procedure gets around this combinatorial explosion of available conformational space by splitting up the seven-helix TM bundle interactions into multiple nearest-neighbor two-helix interactions. All energies are evaluated using the full-atom Dreiding force field (FF) (Mayo, Olafson, & Goddard, 1990).

- 4.1.** Identify nearest-neighbor helix pairs based on the structural template being considered. For a seven-helix TM bundle based on class A GPCRs (Fig. 2.3A), the following 12 pairs of helices specify the nearest-neighbor interactions: H1–H2, H1–H7, H2–H3, H2–H4, H2–H7, H3–H4, H3–H5, H3–H6, H3–H7, H4–H5, H5–H6, and H6–H7 as shown with two-way arrows in Fig. 2.3B.
- 4.2.** For each of the identified helix pairs, a full sampling of helix rotation angles is performed on the 30° grid to generate 144 ($=12 \times 12$) two-helix bundles. During this sampling, the other helices are completely absent (Fig. 2.3C).
- 4.3.** For each of the 144 two-helix bundles from previous step, the residue side chains are optimized by using a rotamer placement method called SCREAM (Kam & Goddard, 2008). This method uses a rotamer library of residue side chain conformations coupled to an MC sampling using full valence, hydrogen bond, and electrostatic interactions, but

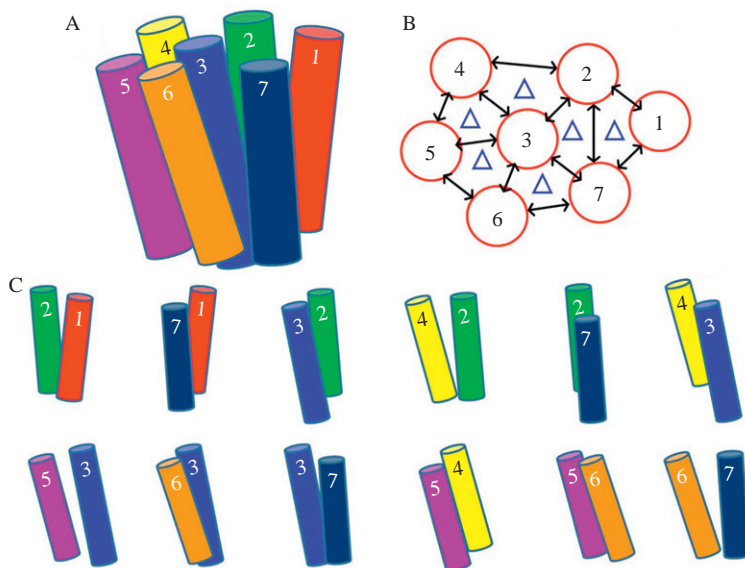


Figure 2.3 (A) Typical seven-helix bundle. (B) Nearest-neighbor helix pairs highlighted by double arrows. (C) The 12-helix pairs are shown explicitly (Abrol, Bray, et al., 2012).

special vdW potentials that reduce the penalty for contacts that are slightly too short while preserving the normal attractive interactions at full strength. This is followed by 10 steps of conjugate-gradient minimization and evaluation of two-helix energies.

- 4.4. The interhelical and intrahelical components of these two-helix energies for each of the 144 two-helix bundle conformations are used to obtain mean-field energies for all possible ~ 35 million TM bundle conformations (Abrol, Bray, et al., 2012).
- 4.5. The energies are ordered and top 2000 TM bundle conformations with lowest energies are output. It is to be noted that since these energies are based on two-helix energies, they provide an approximate ordering of these (seven-helix) TM bundle conformations.
- 4.6. To provide a more accurate energy ordering of these conformations, these TM bundle are explicitly built based on the rotation angles specified for each of the TM helices.
- 4.7. The side chains of the full seven-helix bundle are optimized collectively using SCREAM.

4.8. The resulting bundles are optimized with 10 steps of conjugate-gradient minimization and total energies are evaluated for each bundle using the Dreiding FF, and all conformations ordered by this energy. The above detailed procedure has been applied to six of the GPCR crystal structures and the TM bundle packing observed in the crystal structures was ranked first (had lowest energy) (Abrol, Bray, et al., 2012). The results showed that the energies are reliable to rank all the possible TM bundle conformations in the helix rotation angle η space. An analysis of the lowest energy conformations also provided evidence of other conformations that may be important for GPCR activation. For example, analysis of the 20 lowest energy conformations for rhodopsin showed high energy conformations with rotation angle preferences for TM3 and TM6 consistent with meta rhodopsin II (Abrol, Bray, et al., 2012), the active form of rhodopsin. So, the BiHelix procedure is capable of identifying the correct lowest energy conformations and also other high energy conformations that may be relevant for GPCR activation.

After the application of the BiHelix procedure to a target GPCR starting with multiple structural templates, the conformations with the lowest energy across all templates are taken forward for the more exhaustive TM bundle conformational sampling involving helix tilt, sweep, and rotation angles as described next.



5. SUPERBIHELIX TM BUNDLE SAMPLING OF ALL HELIX ORIENTATION ANGLES

The BiHelix procedure might result in 2–3 low energy but diverse conformations that can be good starting points for sampling helix tilt (θ), sweep (ϕ), rotation (η) angles simultaneously. If one samples, a conformational space of $\pm 10^\circ$ in θ (with $\Delta\theta = 10^\circ$), $\pm 30^\circ$ in ϕ (with $\Delta\phi = 15^\circ$), and $\pm 30^\circ$ in η (with $\Delta\eta = 15^\circ$), it corresponds to $75^7 \sim 10$ trillion TM bundle conformations, for each of which the residue side chains will need to be optimized to obtain the most favorable interactions across the TM bundle being sampled. This is computationally prohibitive and the SuperBiHelix procedure gets around this combinatorial explosion of available conformational space by using the BiHelix concept and splitting up the seven TM bundle interactions into multiple nearest-neighbor two-helix interactions. Except for the large number of two-helix conformations being sampled, the steps involved in SuperBiHelix are identical to those in the BiHelix procedure as described in Section 4, hence they will not be repeated here.

An analysis of the available templates reveals that they differ from each other in all three-helix orientation angles, so the SuperBiHelix procedure was tested to see if it can reproduce the correct template if one started with the wrong template. This was demonstrated by taking the human A_{2A} structure helices and placing them in the human β 2 template to see if the SuperBiHelix procedure could identify the native human A_{2A} crystal conformation. The starting structure had a C α RMSD of 2.1 Å relative to the A_{2A} crystal conformation. After the SuperBiHelix sampling procedure, the lowest energy conformation had an improved C α RMSD of 1.4 Å relative to the crystal conformation (Abrol et al., 2011). More importantly, the improved conformation (after sampling) was able to recognize the correct binding mode of the cocrystallized ligand, whereas the starting structure was not able to. This shows that the exhaustive conformational space sampling of the SuperBiHelix procedure is capable of removing dependence on a given template. It has also been shown that if the sequence similarity of the target protein to the template protein is higher in the TM region, the corresponding conformational space sampling necessary will be smaller and more computationally tractable (Abrol et al., 2011).

At the end of the SuperBiHelix procedure, one typically saves \sim 2000 lowest energy TM bundle conformations and uses the lowest \sim 100 of those for further analysis as described below.



6. EFFECT OF MUTATIONS ON THE WT CONFORMATIONAL ENSEMBLE

Using the lowest \sim 100 conformations from SuperBiHelix, one can determine, to first approximation, the conformations that may be stabilized for a specific receptor mutant.

- 6.1. Use SCREAM to create the specific receptor mutant in each of the \sim 100 SuperBiHelix conformations, by optimizing the specific residue and neighboring residues within 4 Å of the residue being mutated.
- 6.2. Perform 10 steps of conjugate-gradient minimization on each of the mutated \sim 100 TM bundle conformations. Reorder the conformations using the new set of evaluated total energies.

Application of this procedure to human CCR5 chemokine receptor mutants resulted in interesting results, shown for three mutants in Fig. 2.4. It showed, for example, for the W86A mutant, how a high energy WT conformation (wt30) could rank fourth in the mutant, and how the lowest energy WT conformation (wt1) could disappear from the top 20 conformations for

Reordering of CCR5 apo conformations
For W86A, A90H, T105A mutants

W86A	AvgRank	A90H	AvgRank	T105A	AvgRank
wt1	8.0	wt3	3.0	wt1	4.0
wt3	11.8	wt2	6.0	wt3	7.8
wt2	15.0	wt4	15.3	wt2	10.0
wt30	16.0	wt5	16.3	wt11	28.3
wt6	20.8	wt13	18.5	wt9	28.8
wt17	26.0	wt10	21.0	wt12	29.3
wt7	28.3	wt9	22.5	wt18	30.5
wt8	29.3	wt27	22.8	wt4	30.5
wt4	30.0	wt14	23.8	wt27	30.8
wt18	30.3	wt32	24.8	wt6	31.0
wt11	30.3	wt64	25.0	wt7	31.3
wt48	31.0	wt15	25.0	wt20	31.5
wt20	31.3	wt16	25.8	wt8	31.8
wt12	31.3	wt26	27.0	wt14	31.8
wt19	34.8	wt28	27.5	wt13	34.0
wt14	34.8	wt31	28.5	wt15	36.0
wt9	35.8	wt17	29.3	wt5	36.0
wt27	36.0	wt33	30.3	wt64	37.3
wt34	37.0	wt11	32.0	wt32	38.0
wt13	38.0	wt74	32.5	wt30	42.5

Wild type #30 becomes W86A#4

wt1 not in top 20?

40

Figure 2.4 Reordering of wild-type (WT) conformations upon mutations (Abrol & Goddard, 2011).

the A90H mutant. These mutant conformations when docked to CCR5 ligand Maraviroc, resulted in improved correlation with binding assays of Maraviroc to the CCR5 mutants, providing evidence for a large effect of mutations on receptor conformations, which should be taken into account to accurately predict the structural and ligand binding properties.



7. ENSEMBLE DOCKING OF LIGANDS TO WT OR MUTANT RECEPTORS

The following two examples highlight how the ensemble of GPCR conformations predicted by the GEnSeMBLE method for the WT receptor or the mutant receptor (as described in the previous section) can be used to identify specific receptor conformations that may be preferred by different ligands, and which can generate hypothesis about receptor activation.

7.1. Ensemble docking of agonists and antagonists to human A₃ adenosine receptor

The GEnSeMBLE method was used to predict an ensemble of the 20 apo protein predicted structures for the human A₃ adenosine receptor (hAA₃R) (Kim, Riley, Abrol, Jacobson, & Goddard, et al., 2011), as shown in Fig. 2.5A.

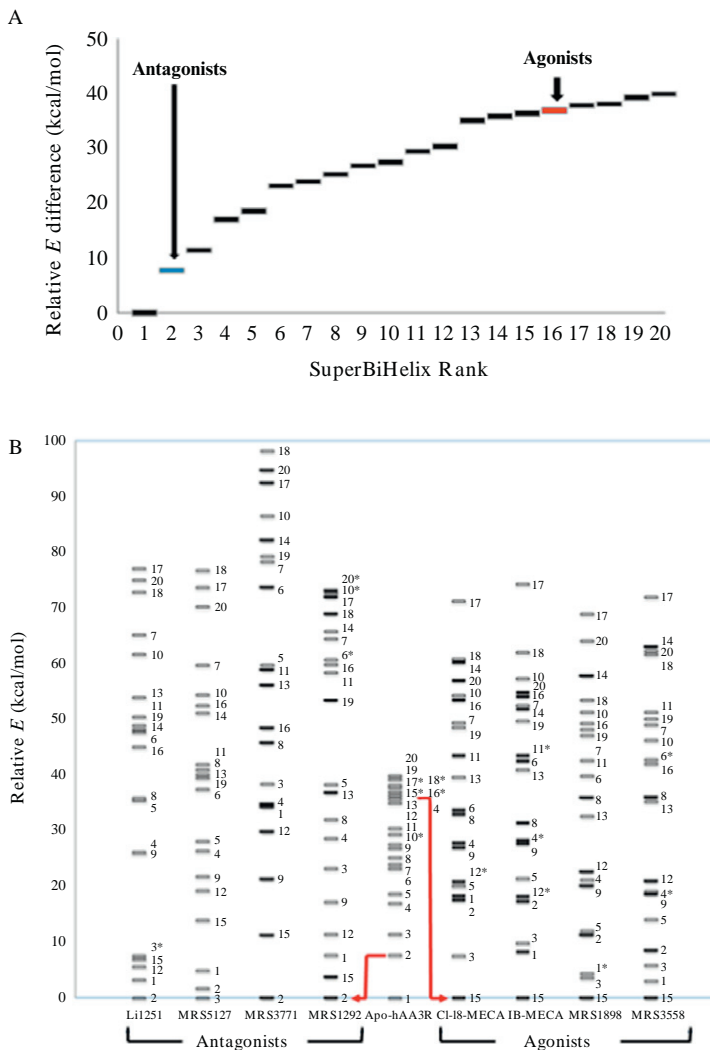


Figure 2.5 Graphical summary of ensemble docking. The relative energies for apo (A) and antagonist- or agonist-bound (B) human A₃ adenosine receptors (hAA₃R) are displayed (Kim et al., 2011).

The hAA₃R selective agonists and selective antagonists were docked to each of the best 20 predicted structures from SuperBiHelix and the receptor conformation preferred by a ligand was identified based on the lowest total energy cocomplex.

As shown in Fig. 2.5B, we find that all four agonists, Cl-IB-MECA, IB-MECA, MRS1898, and MRS3558, prefer to bind to the 15th lowest energy conformation from SuperBiHelix (TMH4 φ : -15° , TMH6 φ : 15° , TMH4 η : -15°).

On the other hand, the three antagonists, MRS3771, LJ1251, and MRS1292 prefer to bind to the second lowest energy conformation (TMH6 φ : 15° , TMH4 η : -15°), whereas antagonist MRS5127 prefers the third lowest energy receptor conformation with TMH4 φ : 15° , TMH6 φ : -30° , TMH4 η : -15° (Fig. 2.5B).

It is expected that the active conformation of the apo receptor has a higher energy than that of the inactive conformation, so agonist is expected (though not always) to show a stronger binding preference for a higher energy receptor conformation as found above. Further analysis of the apo and holo hAA₃R receptor conformations reveals the following. The 20 most stable predicted structures for the apo protein all have a *gauche* + χ_1 rotamer preference for W6.48 (leading to the vertical orientation with respect to the membrane plane) that has been implicated from experiments on other GPCRs to be associated with the inactive form (Cherezov et al., 2007; Jaakola et al., 2008; Warne et al., 2008).

We predicted the bound structure of the agonist (Cl-IB-MECA) to each of these predicted 20 lowest apo-hAA₃R structures and found that the predicted best structure (to apo-15) and 60% of the 20 show a preference of W6.48 for the *trans* χ_1 rotamer (leading to the horizontal orientation with respect to the membrane plane). Previous experiments on other GPCRs have indicated that the *trans* χ_1 rotamer W6.48 maybe involved in activation (Pellissier et al., 2009; Ruprecht, Mielke, Vogel, Villa, & Schertler, 2004).

The predicted rotamer switch of W243^{6,48} induced by binding of the agonist found in this study is consistent with some experimental observations (Gao et al., 2002). Thus, the W243A mutation in hAA₃R dramatically impaired functional coupling but did not diminish agonist affinity. Also W243F affected function but did not diminish agonist affinity. Thus, we conclude that binding the agonist induces reorientation of the W243^{6,48} side chain which affects the receptor's transition from an inactive to an active state.

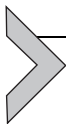
In summary, we find that all four selective agonists prefer what was the 15th predicted structure of the apo protein. In addition, all four change the W6.48 conformational state from *gauche* + (vertical) to *trans* (horizontal). This is consistent with observations in other GPCRs that switching of W6.48 from *gauche* + (vertical) to *trans* (horizontal) is associated with activation of the G protein.

7.2. Ensemble ligand docking to human CCR5 chemokine receptor mutants

Receptor mutagenesis and its effect on ligand binding can reveal details on the ligand binding site. Some mutations affect the protein structure and indirectly affect ligand binding, while others directly affect ligand binding as the ligand would have a direct interaction with the residue being mutated. To probe these effects of mutations, ensembles of human CCR5 mutant receptor conformations were generated as described in the previous section for different mutants shown in Fig. 2.6. As mentioned before, even at the apo conformation level, different mutants stabilize different sets of conformations. Multiple ligands were docked to the lowest energy ensembles of WT and mutant receptor conformations. The results for binding of Maraviroc (the only drug in the market aimed at CCR5) are shown in Fig. 2.6, which shows the different protein conformations preferred by the apo protein and by the Maraviroc bound receptor for different mutants. It was also found that different ligands (Maraviroc, PF-232798, Aplaviroc) prefer different sets of CCR5 conformations, which is consistent with observations that these ligands bind to the same site but show different interaction profiles in mutagenesis studies (Kondru et al., 2008; Maeda et al., 2006) and in effects on antibody binding (Kenakin, 2007).

Mutations	CCR5 Confs	
	Apo	Mara
Wild-type	wt1	wt7
F109Y	wt3	wt5
F112A	wt1	wt5
Q194A	wt1	wt5
Y251F	wt1	wt2
D276A	wt1	wt2
Q277A	wt1	wt5
W86A	wt1	wt3
A90H	wt3	wt10
T105A	wt1	wt2
Y108A	wt3	wt2
F109A	wt1	wt5
I198A	wt1	wt5
Y251A	wt2	wt3
Q280A	wt3	wt5
E283A	wt3	wt3

Figure 2.6 Reordering of wild-type CCR5 conformations for various mutants and the conformation preferred by Maraviroc for each of the mutants (Abrol & Goddard, 2011).



8. SUMMARY

The conformational ensemble view of GPCRs, which has been validated by numerous biophysical and functional studies, when coupled to structural studies is providing detailed mechanistic insights into the functional selectivity of GPCRs. This, in turn, is presenting new drug targeting mechanisms that may eventually lead to therapeutics with minimal side effects. The computational approaches (like the GEnSeMBLE method) when combined with structural and functional data on these receptors are beginning to generate a dynamical and thermodynamic framework of these receptors (Fig. 2.1), where different subsets of receptor conformations are stabilized under different conditions (receptor mutants or ligand binding, etc.). Different mutants and ligands can be used to probe the activation landscape of these receptors. Combined with the exponential increase in available GPCR structures, this is generating novel insights and rich hypotheses on the atomic level mechanisms behind GPCR activation and function.

ACKNOWLEDGMENTS

This work was supported in part by the NIH Grant 5R21MH073910, by funding from PharmSelex, and by gifts to the Materials and Process Simulation Center at Caltech.

REFERENCES

- Abrol, R., Bray, J. K., & Goddard, W. A. (2012). Bihelix: Towards de novo structure prediction of an ensemble of G-protein coupled receptor conformations. *Proteins: Structure, Function, and Bioinformatics*, 80(2), 505–518.
- Abrol, R., & Goddard, W. A., 3rd (2011). G protein-coupled receptors: Conformational ‘gatekeepers’ of transmembrane signal transduction and diversification. In J. D. Adams & K. K. Parker (Eds.), *Extracellular and intracellular signalling* (pp. 188–229). Cambridge: RSC.
- Abrol, R., Griffith, A. R., Bray, J. K., & Goddard, W. A. (2012). Structure prediction of G protein-coupled receptors and their ensemble of functionally important conformations. In N. Vaidehi & J. Klein-Seetharaman (Eds.), *Membrane protein structure: Methods and protocols*, Vol. 914, (pp. 237–254). New York: Humana.
- Abrol, R., Kim, S. K., Bray, J. K., Griffith, A. R., & Goddard, W. A. (2011). Characterizing and predicting the functional and conformational diversity of seven-transmembrane proteins. *Methods*, 55(4), 405–414.
- Ballesteros, J. A., & Weinstein, H. (1995). Integrated methods for the construction of three dimensional models and computational probing of structure function relations in G protein-coupled receptors. In S. C. Sealfon & P. M. Conn (Eds.), *Methods in neuroscience*, Vol. 25, (pp. 366–428). San Diego: Academic Press.
- Blois, T. M., & Bowie, J. U. (2009). G-protein-coupled receptor structures were not built in a day. *Protein Science*, 18(7), 1335–1342.

- Cherezov, V., Rosenbaum, D. M., Hanson, M. A., Rasmussen, S. G., Thian, F. S., Kobilka, T. S., et al. (2007). High-resolution crystal structure of an engineered human beta2-adrenergic G protein-coupled receptor. *Science*, *318*(5854), 1258–1265.
- Chien, E. Y. T., Liu, W., Zhao, Q. A., Katritch, V., Han, G. W., Hanson, M. A., et al. (2010). Structure of the human dopamine D3 receptor in complex with a D2/D3 selective antagonist. *Science*, *330*(6007), 1091–1095.
- Choe, H. W., Kim, Y. J., Park, J. H., Morizumi, T., Pai, E. F., Krauss, N., et al. (2011). Crystal structure of metarhodopsin II. *Nature*, *471*(7340), 651–655.
- Deupi, X., & Kobilka, B. K. (2010). Energy landscapes as a tool to integrate GPCR structure, dynamics, and function. *Physiology*, *25*(5), 293–303.
- Gao, Z. G., Chen, A., Barak, D., Kim, S. K., Muller, C. E., & Jacobson, K. A. (2002). Identification by site-directed mutagenesis of residues involved in ligand recognition and activation of the human A(3) adenosine receptor. *The Journal of Biological Chemistry*, *277*(21), 19056–19063.
- Haga, K., Kruse, A. C., Asada, H., Yurugi-Kobayashi, T., Shiroishi, M., Zhang, C., et al. (2012). Structure of the human M2 muscarinic acetylcholine receptor bound to an antagonist. *Nature*, *482*(7386), 547–551.
- Hanson, M. A., Roth, C. B., Jo, E. J., Griffith, M. T., Scott, F. L., Reinhart, G., et al. (2012). Crystal structure of a lipid G protein-coupled receptor. *Science*, *335*(6070), 851–855.
- Heo, J., Han, S. K., Vaidehi, N., Wendel, J., Kekenus-Huskey, P., & Goddard, W. A., 3rd (2007). Prediction of the 3D structure of FMRF-amide neuropeptides bound to the mouse MrgC11 GPCR and experimental validation. *ChemBioChem*, *8*(13), 1527–1539.
- Jaakola, V. P., Griffith, M. T., Hanson, M. A., Cherezov, V., Chien, E. Y., Lane, J. R., et al. (2008). The 2.6 angstrom crystal structure of a human A2A adenosine receptor bound to an antagonist. *Science*, *322*(5905), 1211–1217.
- Kam, V. W. T., & Goddard, W. A. (2008). Flat-bottom strategy for improved accuracy in protein side-chain placements. *Journal of Chemical Theory and Computation*, *4*(12), 2160–2169.
- Kenakin, T. (2007). Collateral efficacy in drug discovery: Taking advantage of the good (allosteric) nature of 7TM receptors. *Trends in Pharmacological Sciences*, *28*(8), 407–415.
- Kenakin, T. P. (2012). Biased signalling and allosteric machines: New vistas and challenges for drug discovery. *British Journal of Pharmacology*, *165*(6), 1659–1669.
- Kenakin, T., & Miller, L. J. (2010). Seven transmembrane receptors as shape shifting proteins: The impact of allosteric modulation and functional selectivity on new drug discovery. *Pharmacological Reviews*, *62*(2), 265–304.
- Kim, S.-K., Riley, L., Abrol, R., Jacobson, K. A., & Goddard, W. A., 3rd (2011). Predicted structures of agonist and antagonist bound complexes of adenosine A₃ receptor. *Proteins: Structure, Function, and Bioinformatics*, *79*(6), 1878–1897.
- Kondru, R., Zhang, J., Ji, C., Mirzadegan, T., Rotstein, D., Sankuratri, S., et al. (2008). Molecular interactions of CCR5 with major classes of small-molecule anti-HIV CCR5 antagonists. *Molecular Pharmacology*, *73*(3), 789–800.
- Kruse, A. C., Hu, J. X., Pan, A. C., Arlow, D. H., Rosenbaum, D. M., Rosemond, E., et al. (2012). Structure and dynamics of the M3 muscarinic acetylcholine receptor. *Nature*, *482*(7386), 552–556.
- Lagerstrom, M. C., & Schioth, H. B. (2008). Structural diversity of G protein-coupled receptors and significance for drug discovery. *Nature Reviews. Drug Discovery*, *7*(4), 339–357.
- Li, Y., Zhu, F., Vaidehi, N., Goddard, W. A., 3rd, Sheinerman, F., Reiling, S., et al. (2007). Prediction of the 3D structure and dynamics of human DP G-protein coupled receptor bound to an agonist and an antagonist. *Journal of the American Chemical Society*, *129*(35), 10720–10731.

- Lomize, M. A., Lomize, A. L., Pogozheva, I. D., & Mosberg, H. I. (2006). OPM: Orientations of proteins in membranes database. *Bioinformatics*, *22*(5), 623–625.
- Maeda, K., Das, D., Ogata-Aoki, H., Nakata, H., Miyakawa, T., Tojo, Y., et al. (2006). Structural and molecular interactions of CCR5 inhibitors with CCR5. *The Journal of Biological Chemistry*, *281*(18), 12688–12698.
- Mayo, S. L., Olafson, B. D., & Goddard, W. A. (1990). Dreiding—A generic force-field for molecular simulations. *The Journal of Physical Chemistry*, *94*(26), 8897–8909.
- Palczewski, K., Kumasaka, T., Hori, T., Behnke, C. A., Motoshima, H., Fox, B. A., et al. (2000). Crystal structure of rhodopsin: A G protein-coupled receptor. *Science*, *289*(5480), 739–745.
- Pellissier, L. P., Sallander, J., Campillo, M., Gaven, F., Queffeuilou, E., Pillot, M., et al. (2009). Conformational toggle switches implicated in basal constitutive and agonist-induced activated states of 5-hydroxytryptamine-4 receptors. *Molecular Pharmacology*, *75*(4), 982–990.
- Rajagopal, K., Lefkowitz, R. J., & Rockman, H. A. (2005). When 7 transmembrane receptors are not G protein-coupled receptors. *The Journal of Clinical Investigation*, *115*(11), 2971–2974.
- Rasmussen, S. G., DeVree, B. T., Zou, Y., Kruse, A. C., Chung, K. Y., Kobilka, T. S., et al. (2011). Crystal structure of the beta2 adrenergic receptor-Gs protein complex. *Nature*, *477*(7366), 549–555.
- Rosenbaum, D. M., Rasmussen, S. G., & Kobilka, B. K. (2009). The structure and function of G-protein-coupled receptors. *Nature*, *459*(7245), 356–363.
- Ruprecht, J. J., Mielke, T., Vogel, R., Villa, C., & Schertler, G. F. X. (2004). Electron crystallography reveals the structure of metarhodopsin I. *The EMBO Journal*, *23*(18), 3609–3620.
- Shukla, A. K., Xiao, K. H., & Lefkowitz, R. J. (2011). Emerging paradigms of beta-arrestin-dependent seven transmembrane receptor signaling. *Trends in Biochemical Sciences*, *36*(9), 457–469.
- Stevens, R. C., Shimamura, T., Shiroishi, M., Weyand, S., Tsujimoto, H., Winter, G., et al. (2011). Structure of the human histamine H(1) receptor complex with doxepin. *Nature*, *475*(7354), 65–70.
- Tate, C. G., & Stevens, R. C. (2010). Growth and excitement in membrane protein structural biology. *Current Opinion in Structural Biology*, *20*(4), 399–400.
- Vaidehi, N., Schlyer, S., Trabanino, R. J., Floriano, W. B., Abrol, R., Sharma, S., et al. (2006). Predictions of CCR1 chemokine receptor structure and BX 471 antagonist binding followed by experimental validation. *The Journal of Biological Chemistry*, *281*(37), 27613–27620.
- Walters, R. W., Shukla, A. K., Kovacs, J. J., Violin, J. D., DeWire, S. M., Lam, C. M., et al. (2009). beta-Arrestin1 mediates nicotinic acid-induced flushing, but not its antilypolytic effect, in mice. *The Journal of Clinical Investigation*, *119*(5), 1312–1321.
- Warne, T., Serrano-Vega, M. J., Baker, J. G., Moukhametzianov, R., Edwards, P. C., Henderson, R., et al. (2008). Structure of a beta1-adrenergic G-protein-coupled receptor. *Nature*, *454*(7203), 486–491.
- Wu, B. L., Chien, E. Y. T., Mol, C. D., Fenalti, G., Liu, W., Katritch, V., et al. (2010). Structures of the CXCR4 chemokine GPCR with small-molecule and cyclic peptide antagonists. *Science*, *330*(6007), 1066–1071.
- Xu, F., Wu, H. X., Katritch, V., Han, G. W., Jacobson, K. A., Gao, Z. G., et al. (2011). Structure of an agonist-bound human A(2A) adenosine receptor. *Science*, *332*(6027), 322–327.